Anal. Chem. **1998,** *70,* 792−800

In Situ Electrochemical EPR Studies of Charge Transfer across the Liquid/Liquid Interface

Richard D. Webster, Robert A. W. Dryfe,† Barry A. Coles, and Richard G. Compton*

Physical & Theoretical Chemistry Laboratory, Oxford University, South Parks Road, Oxford OX1 3QZ, United Kingdom

The in situ measurement of EPR spectra of radical ions generated at the polarized liquid/liquid interface is described in relation to the 7,7,8,8-tetracyanoquinodimethane (TCNQ), 2,3,5,6-tetrachloro-*p*-benzoquinone (TCBQ), and 2,3,5,6-tetrafluoro-*p*-benzoquinone (TFBQ) radical anions and the tetrathiafulvalene (TTF) radical cation. TCNQ and TTF were chosen as model compounds with which to quantify the performance of a novel liquid/liquid electrochemical EPR cell. The anion radical of TCNQ and the cation radical of TTF in 1,2-dichloroethane (DCE) were produced at the water interface by electron transfer from/to the aqueous-phase ferricyanide/ferrocyanide redox couple by applying a potential difference between the two phases with a four-electrode potentiostat. The EPR signal intensity (at constant magnetic field) of the resultant organic radicals was monitored during potential step experiments which indicated that the EPR data could be modeled in terms of diffusional transport. TCBQ and TFBQ were chosen as compounds to model the electron transfer behavior of biologically important quinones at the oil/water interface. The EPR and voltammetric data obtained from TCBQ/TCBQ$^{-\bullet}$ and TFBQ/TFBQ$^{-\bullet}$ indicated unambiguously that the two semiquinones are stable at the DCE/water interface and do not undergo immediate protonation.

Charge transfer at the liquid/liquid interface has long been recognized to play an important role in certain biological and industrial processes, such as cell membrane energetics and metal extraction.[1] Direct electrochemical studies of the interface between two immiscible electrolyte solutions (ITIES) were transformed when it was discovered that the Galvani potential difference across this interface could be controlled externally.[2] Since this discovery, reactions involving the transfer of both ions and electrons across the ITIES have been studied extensively, with amperometric techniques generally being employed to characterize the interfacial process.[3]

Electron transfer at the ITIES represents an intermediate case between bimolecular homogeneous electron transfer and "conventional" heterogeneous electron transfer at the solid electrode/solution interface.[4] The reaction at the ITIES is bimolecular since it involves the exchange of electron(s) between two species in different phases, but the reaction may also be controlled through alteration of the interfacial potential difference. It has also been noted that the electron transfer is frequently complicated by associated ion-transfer reactions,[5] as one (or more) of the products of the electron-transfer reaction may change phase once generated. It is with these points in mind that effort has been directed toward the development of spectroelectrochemical techniques that would provide an independent means of monitoring charge-transfer reactions, while allowing selective identification of the participating species. A variety of spectroscopic experiments have been used successfully to clarify processes at the metal/electrolyte and semiconductor/electrolyte interfaces.[6] To date, both UV−visible absorption[7] and luminescence spectroscopy[8] have been used in total internal reflection mode to investigate ion transfer across the ITIES. Dynamic luminescent studies have also been applied to the measurement of photoinduced electron transfer at the liquid/liquid interface.[9] Second harmonic techniques have been employed at the ITIES due to their intrinsic surface specificity, which has led to information about fundamental interfacial properties being extracted.[10]

EPR spectroscopy has been used widely in conjunction with electrochemistry at the metal/solution interface due to its selectivity toward paramagnetic species, and in combination with voltammetric data, spectroelectrochemical experiments have permitted the mechanistic resolution of various complex electrochemical reactions.[11] A study of the application of in situ EPR spectroscopy to the ITIES is reported in this paper, which builds on our preliminary communication which described the design and operation of an in situ liquid/liquid electrochemical EPR cell.[12]

† Present address: Department of Chemistry, UMIST, P.O. Box 88, Manchester M60 1QD, United Kingdom.

(1) Girault, H. H.; Schiffrin, D. J. In *Electroanalytical Chemistry*; Bard, A. J., Ed.; Marcel Dekker: New York, 1989; Vol. 15, p 1.
(2) Gavach, C.; Mlodnicka, T.; Guastalla, J. *Compt. Rend. Acad. Sci. Ser. C* **1968**, *266*, 1196.
(3) Girault, H. H. In *Modern Aspects of Electrochemistry*; Bockris, J. O'M.; Conway, B. E., White, R. E., Eds.; Plenum Press: New York, 1993; Vol. 25, p 1.
(4) Marcus, R. A. *J. Phys. Chem.* **1990**, *94*, 1050.
(5) Cunnane, V. J.; Geblewicz, G.; Schiffrin, D. J. *Electrochim. Acta* **1995**, *40*, 3005.
(6) Gale R. J.; Ed. *Spectroelectrochemistry*; Plenum Press: New York, 1988.
(7) Ding, Z.; Wellington, R. G.; Brevet P.-F.; Girault, H. H. *J. Electroanal. Chem.* **1997**, *420*, 35.
(8) Kakiuchi, T.; Takasu, Y.; Senda, M. *Anal. Chem.* **1992**, *64*, 3096. Kakiuchi, T.; Takasu, Y. *Anal. Chem.* **1994**, *66*, 1853. Kakiuchi, T.; Takasu, Y. *J. Electroanal. Chem.*, **1994**, *365*, 293. Kakiuchi, T.; Takasu, Y. *J. Electroanal. Chem.* **1995**, *381*, 5. Ding, Z.; Wellington, R. G.; Brevet, P.-F.; Girault, H. H. *J. Phys. Chem.* **1996**, *100*, 10658.
(9) Dryfe, R. A. W.; Ding, Z.; Wellington, R. G.; Brevet, P.-F.; Kuznetzov. A. M.; Girault, H. H. *J. Phys. Chem. A* **1997**, *101*, 2519.
(10) Naujok, R. R.; Higgins, D. A.; Hanken, D. G.; Corn, R. M. *J. Chem. Soc., Faraday Trans.* **1995**, *91*, 1411. Tamburello Luca, A. A.; Hébert, P.; Brevet, P.-F.; Girault, H. H. *J. Chem. Soc., Faraday Trans.* **1995**, *91*, 1763. Conboy, J. C.; Richmond, G. L. *J. Phys. Chem. B* **1997**, *101*, 983.

S0003-2700(97)00814-7 CCC: $15.00
Published on Web 01/21/1998

In the experiments detailed in this paper we have used 7,7,8,8-tetracyanoquinodimethane (TCNQ) and tetrathiafulvalene (TTF) as model compounds in order that the radical products formed following electron transfer at the water/1,2-dichloroethane (DCE) interface could be monitored by in situ EPR spectroscopy so that the performance of the liquid/liquid EPR cell could be quantified. TCNQ and TTF can be reduced or oxidized respectively by one electron to form stable anion ($TCNQ^{-\bullet}$) or cation ($TTF^{+\bullet}$) radicals.

The behavior of quinones and semiquinones at the oil/water interface is of particular interest because their redox behavior is extremely sensitive to their solution environment. In protic solvents, quinones generally undergo a two- electron−two-proton reduction to the associated hydroquinone (QH_2), whereas two successive one-electron reductions (to the semiquinone radical anion, $Q^{-\bullet}$ and the dianion, Q^{2-}) are seen both in aprotic solvents and in protic media under basic conditions (pH > 2).[13] Quinones are also of interest because of their widespread occurrence in a variety of biological electron-transfer processes, for example, in the mitochondrial chain.[14] Spectroscopic methods, such as EPR[15] and resonance Raman techniques,[16] have been applied to ubiquinone molecules in attempts to rationalize the redox chemistry in terms of the molecular environment. For example, ubiquinones in *Rhodobacter sphaeroides* photosynthetic reaction centers form either the corresponding semiquinone radical anion or the hydroquinone, depending on their position within the protein.[17]

However, the voltammetric behavior of a quinone dissolved in an oil at the water interface is difficult to predict as it is possible that two different reactions could occur: either (i) the semiquinone produced by one-electron reduction is immediately protonated at the water interface or (ii) the semiquinone is not protonated and is able to diffuse from the interface into the bulk oil phase. Electrochemical and EPR experiments allow the discrimination between the two mechanistic pathways by measuring the number of electrons transferred during the reduction of the quinone in the former case, and in the latter case, by measuring the hyperfine structure and intensity of the EPR signal of the reduced product(s). Unfortunately, many biologically important quinones are reduced at potentials outside the range accessible by liquid/liquid electrochemistry due to the interference of ion-transfer processes at very negative or very positive potentials. Therefore, to mimic the liquid/liquid redox behavior of a biological quinone dissolved in a fat at the water interface, we have chosen 2,3,5,6-tetrachloro-*p*-benzoquinone (TCBQ) and 2,3,5,6-tetrafluoro-*p*-benzoquinone (TFBQ) as model compounds dissolved in DCE. Both TCBQ and TFBQ are suitable for electron-transfer studies at the ITIES because they partition preferentially to the oil phase (DCE), are easily reduced, and form stable radical anions. TCBQ has previously been used as an oxidant of ascorbic acid at the ITIES,[18] while its reduction by potassium ferrocyanide in dimethyl sulfoxide/water mixtures has been investigated by UV−visible absorption spectroscopy.[19]

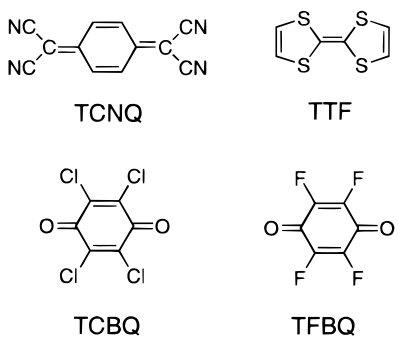

Figure 1. Structures of the organic-phase molecules.

EXPERIMENTAL SECTION

Chemicals and Reagents. The organic phase reagents 7,7,8,8-tetracyanoquinodimethane (98%), tetrathiafulvalene (97%), 2,3,5,6-tetrachloro-*p*-benzoquinone (99%), and 2,3,5,6-tetrafluoro-*p*-benzoquinone (97%) were purchased from Aldrich and used as received (molecular structures are given in Figure 1). The organic phase supporting electrolyte used principally for this study, bis(triphenylphosphoranylidene)ammonium tetrakis(4-chlorophenyl)borate ($BTPPA^+TCPB^-$), was prepared from bis(triphenylphosphoranylidene) ammonium chloride (Aldrich, 97%) and potassium tetrakis(4-chlorophenyl)borate (Fluka, 98%) according to a literature method.[20] A similar procedure was employed in the synthesis of tetraphenylarsonium tetrakis(4-chlorophenyl)borate ($TPhAs^+TCPB^-$), from tetraphenylarsonium chloride (Aldrich, 97%) and potassium tetrakis(4-chlorophenyl)borate. Tetrabutylammonium hexafluorophosphate (n-Bu_4NPF_6; Fluka, electrochemical grade) was used in several experiments to avoid problems associated with the photoinduced oxidation of tetraphenylborate derivatives. HPLC-grade 1,2-dichloroethane (Sigma-Aldrich), and UHQ-grade water of a resistivity not less than 18 MΩ·cm obtained from an Elgastat system (High Wycombe, Bucks, U.K.), were mutually saturated before use. Analytical-grade potassium ferrocyanide and potassium ferricyanide were supplied by BDH chemicals.

Procedures for Liquid/Liquid Interfacial Measurements. The cell used to perform the interfacial polarization EPR experi-

(11) (a) Goldberg, I. R.; Bard, A. J. *J. Phys. Chem.* **1974**, *78*, 290. (b) Goldberg, I. R.; Boyd, D.; Hirasawa, R.; Bard, A. J. *J. Phys. Chem.* **1974**, *78*, 295. (c) Waller, A. M.; Compton, R. G. *Comp. Chem. Kinet.* **1989**, *29*, 297. (d) Compton, R. G.; Dryfe, R. A. W. *Prog. React. Kinet.* **1995**, *20*, 245. (e) Allendoerfer, R. D.; Martinchek, G. A.; Brukenstein, S. *Anal. Chem.* **1975**, *47*, 890−894. (f) Compton, R. G.; Coles, B. A. *J. Electroanal. Chem.* **1983**, *144*, 87. (g) Fiedler, D. A.; Koppenol, M.; Bond, A. M. *J. Electrochem. Soc.* **1995**, *142*, 862. (h) Webster, R. D.; Bond, A. M.; Coles, B. A.; Compton, R. G. *J. Electroanal. Chem.* **1996**, *404*, 303−308. (i) Webster, R. D.; Bond, A. M.; Schmidt, T. *J. Chem. Soc., Perkin Trans. 2* **1995**, 1365. (j) Compton, R. G.; Waller, A. M. In *Spectroelectrochemistry: Theory and Practice*; Gale, R. J., Ed.; Plenum Press: New York, 1988; Chapter 7.

(12) Dryfe, R. A. W.; Webster, R. D.; Coles B. A.; Compton, R. G. *J. Chem. Soc., Chem. Commun.* **1997**, 779.

(13) Chambers, J. Q. In *The Chemistry of Quinoid Compounds*; Patai, S., Ed.; Wiley: New York, 1974; Vol. 1, Chapter 14, p 737. Chambers, J. Q. In *The Chemistry of Quinoid Compounds*; Patai, S., Rappoport, Z., Eds.; Wiley: New York, 1988, Vol. 2, Chapter 12, p 719. Gupta, N.; Linschitz, H. *J. Am. Chem. Soc.* **1997**, *119*, 6384−6391.

(14) Tyler, D. D. *The Mitochondrion in Health and Disease*; VCH: New York, 1992; p 284.

(15) Joela, H.; Kasa, S.; Lehtovuori, P.; Bech, M. *Acta Chem. Scand.* **1997**, *51*, 233.

(16) Zhao, X.; Ogura, T.; Okamura, M.; Kitagawa, T. *J. Am. Chem. Soc.* **1997**, *119*, 5263.

(17) Paddock, M. L.; McPherson, P. L.; Feher, P. M.; Okamura, M. Y. *Proc. Natl. Acad. Sci. U.S.A.* **1990**, *87*, 6803.

(18) Suzuki, M.; Umetani, S.; Matsui, M.; Kihara, S. *J. Electroanal. Chem.* **1997**, *420*, 119.

(19) Girgis, M. M.; Osman, A. H.; Arifien, A. E. *Indian J. Chem.* **1991**, *30A*, 235.

(20) Osborne, M. D.; Shao, Y.; Pereira, C. M.; Girault, H. H. *J. Electroanal. Chem.* **1994**, *364*, 155.

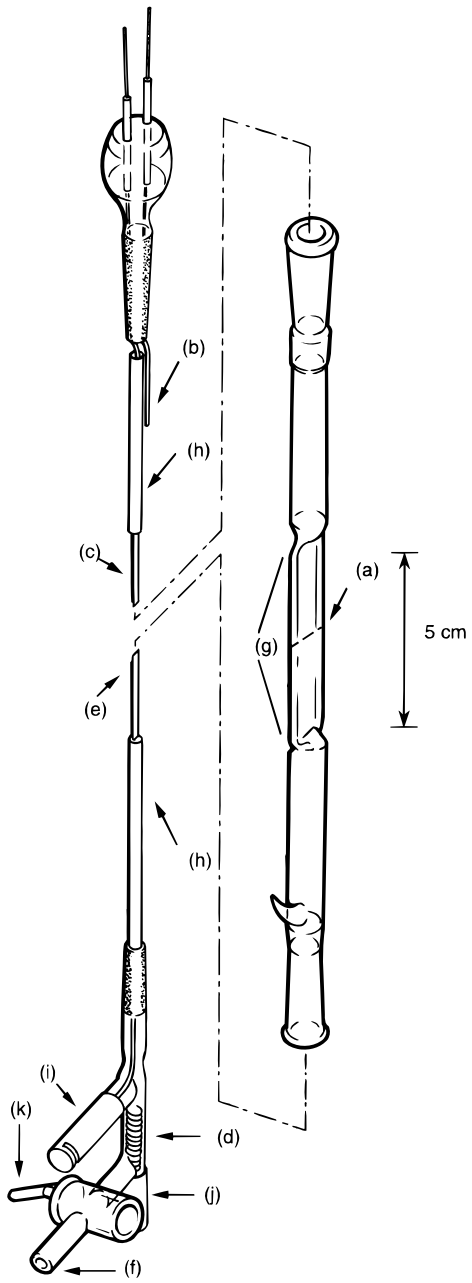

Figure 2. Silica cell for performing liquid/liquid electrochemical EPR experiments: (a) interface between two immiscible liquids, (b) platinum wire counter electrode 1, (c) silver wire reference electrode 1, (d) platinum wire counter electrode 2, (e) silver wire reference electrode 2, (f) capillary to fill lower portion of cell, (g) thin-layer portion of cell, (h) Teflon/silicone rubber sleeves surrounding lower portions of reference electrodes, (i) electrical contact to reference electrode 2, (j) electrical contact to counter electrode 2, and (k) ground glass tap. Adapted from Figure 1, ref 12.

ments is shown in Figure 2 and is essentially a conventional silica flat cell[21] (Bruker WG-812 ER 160 FC) modified so that a counter and a reference electrode can be inserted into either end. The cell was assembled by first filling the higher density solvent (DCE) through the capillary at the base of the cell (Figure 2f) so that the solvent reached the midpoint of the flat portion of the cell (Figure 2a) and then sealing the capillary with a tap (Figure 2k). The upper, less dense phase (water) was then introduced into the cell from the top using a Pasteur pipet. With this filling method, a liquid/liquid interface could be generated and maintained in the midportion of the flat part of the cell.

The cell was connected to a four-electrode potentiostat, designed and built in-house, to allow the imposition of a potential difference across the ITIES relative to the two reference electrodes used, with the circuit being completed by current flow through the two counter electrodes.[22] An external input was added to the computer-controlled potentiostat so that the EPR data could be collected simultaneously (as dc output from the EPR spectrometer) with the current and signal data recorded as a function of time during potential step experiments. The two counter electrodes of coiled 0.5-mm-diameter platinum wire were located outside the thin-layer section (Figure 2b and d) to avoid contamination in the flat part of the cell from any paramagnetic species produced at the counter electrodes. The two reference electrodes were 0.5-mm-diameter silver wires, flattened at one end to a thickness that enabled their insertion into the flat part of the cell (Figure 2c and e). The inherent high resistivity of the organic phase, due to the low relative permittivity of the solvent used (DCE), is exacerbated by the thin-layer cell geometry. Therefore, to minimize ohmic loss and to improve control over the potential difference applied between the liquid phases, both silver pseudoreference electrodes were positioned in very close proximity (<5 mm) to the liquid/liquid interface. Furthermore, the portions of the reference electrodes outside the flat part of the cell were jacketed in Teflon tubing (Figure 2h) and sealed with silicone rubber so that they were only in contact with the solutions inside the flat part of the cell. For purely electrochemical experiments, a cylindrical cell with an interfacial diameter of 1 cm and two Luggin capillaries was employed.[23]

Electrolysis Experiments. Controlled-potential bulk electrolysis experiments were conducted in DCE with 0.1 M *n*-Bu_4PF_6 using a two-compartment electrolysis cell similar to that described previously.[11i] The working and counter electrodes were platinum mesh and the reference electrode was an Ag/Ag^+ (0.05 M $AgNO_3$). Typical electrolysis times for a one-electron bulk reduction or oxidation of a 5 mM solution of analyte was approximately 30 min. The data for the fraction of electrons transferred was calculated from

$$N = Q/nF \qquad (1)$$

where N is the number of moles, Q is the integrated charge passed, n is the number of electrons, and F is the Faraday constant. The data were calibrated in order to take into account the effect of background current on the overall measured charge.

In situ electrochemical EPR experiments were conducted on 5 mM concentration solutions of the analytes in DCE with 0.1 M *n*-Bu_4NPF_6 using a three-electrode stationary solution electrochemical cell that has been described previously.[11g]

EPR Measurements. Continuous-wave first-derivative X-band EPR spectra were recorded on a Bruker ER 200D spectrometer operating with a TE_{102} cavity. In all cases the modulation

(21) Piette, L. H.; Ludwig P.; Adams, R. N. *Anal. Chem.* **1962**, *34*, 916. Piette, L. H.; Ludwig P.; Adams, R. N. *Anal. Chem.* **1962**, *34*, 1587.

(22) Samec, Z.; Marecek, V.; Weber, J. *J. Electroanal. Chem.* **1979**, *100*, 841.
(23) Shao, Y.; Girault, H. H. *J. Electroanal. Chem.* **1990**, *282*, 59.

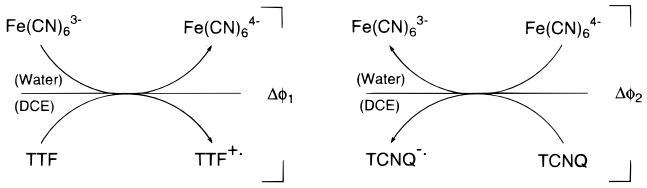

Figure 3. Reaction schemes for the potential-induced interfacial oxidation of TTF (oil phase) by potassium ferricyanide (aqueous phase) and reduction of TCNQ (oil phase) by potassium ferrocyanide (aqueous phase).

frequency was 100 kHz, the time constant was 5 ms, and for field sweep experiments the sweep time was 100 s.

RESULTS AND DISCUSSION

(1) Liquid/Liquid Voltammetric and EPR Studies on TCNQ and TTF and Their Associated Anion or Cation Radicals. The two reactions initially selected as model ITIES electron-transfer systems were the reduction of DCE-phase TCNQ (to $TCNQ^{-\bullet}$) by aqueous-phase potassium ferrocyanide and the oxidation of DCE-phase TTF (to $TTF^{+\bullet}$) by aqueous-phase potassium ferricyanide (Figure 3). The liquid/liquid TCNQ/ferrocyanide system was previously investigated using electrochemical means, which have indicated that the charge-transfer process observed on polarization of the liquid/liquid interface is due to heterogeneous reduction of TCNQ by the aqueous couple.[24] A similar mechanism can be written for the oxidation of TTF by ferricyanide,[24a] as shown in Figure 3, where $\Delta\phi_1$ and $\Delta\phi_2$ denote a potential difference applied across the water/DCE interface.

A preliminary experiment consisted of the ex situ variation of $\Delta\phi$ through control of the partitioning of a common ion. The resultant Nernst−Donnan equilibrium is given by

$$\Delta_o^w \phi = \Delta_o^w \phi^o + \frac{RT}{nF} \ln \frac{a_i(o)}{a_i(w)} \qquad (2)$$

where the superscript represents the standard interfacial potential difference induced by the partitioning of the common ion, *i*. In this case, the ion used was the tetraphenylarsonium cation, present as its tetrakis(4-chlorophenyl)borate salt in the DCE phase, and as its chloride salt in the aqueous phase. It was noted by Solomon and Bard,[24c] that adjustment of the relative concentrations of the salts can be used to drive the interfacial TCNQ/ferrocyanide electron transfer "uphill" because the difference in the standard reduction potentials of the TCNQ and ferrocyanide couples (−0.19 V) is overcome by the interfacial potential difference induced by equal activities of the $TPhAs^+$ (−0.36 V). Accordingly, a solution of 0.2 mM TCNQ and 10 mM $TPhAs^+TPBCl^-$ in DCE was shaken with an aqueous solution of 1 mM potassium ferrocyanide and 10 mM $TPhAs^+Cl^-$. An immediate color change from yellow-green to deep blue-green was observed in the organic phase and on transfer to the silica EPR cell, a single-line EPR signal with a peak-to-peak line width (ΔH_{pp}) of 0.5 mT was detected, which appears to be typical of $TCNQ^{-\bullet}$ radical in DCE.

(24) (a) Kihara, S.; Suzuki, M.; Maeda, K.; Ogura, K.; Matsui, M.; Yoshida, Z. *J. Electroanal. Chem.* **1989**, *271*, 107. (b) Cheng Y.; Schiffrin, D. J. *J. Chem. Soc., Faraday Trans.* **1994**, *90*, 2517. (c) Solomon T.; Bard, A. J. *J. Phys. Chem.* **1995**, *99*, 17487.

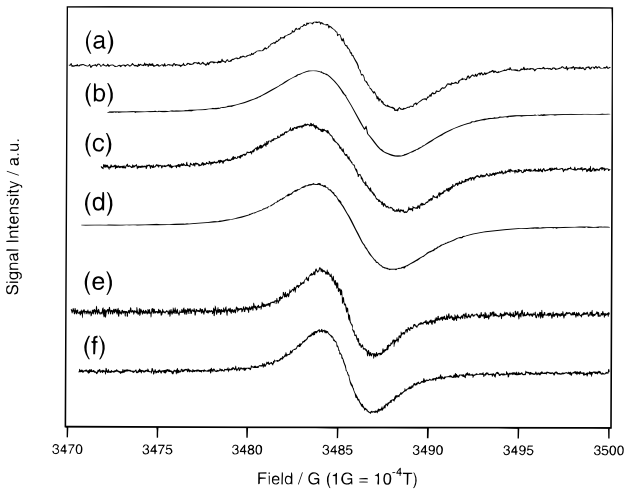

Figure 4. EPR spectra obtained in DCE by (a) in situ electrolysis in an electrochemical EPR cell (see Experimental Section) of 4.9 mM TCNQ with 0.1 M *n*-Bu_4NPF_6. EPR modulation amplitude, 0.02 mT. (b) Exhaustive electrolysis of a 5.3 mM solution of TCNQ with 0.1 M *n*-Bu_4NPF_6 in a controlled-potential electrolysis cell, and then the solution transferred into a silica flat cell for EPR measurements. EPR modulation amplitude, 0.01 mT. (c) The same solution in (b) that was diluted with DCE by a factor of 50 to give 0.1 mM $TCNQ^{-\bullet}$ and 2 mM *n*-Bu_4NPF_6. EPR modulation amplitude, 0.05 mT. (d) In situ electrolysis in a liquid/liquid electrochemical-EPR cell, by polarization of the water/DCE interface of 5.4 mM TCNQ with 50 mM $BTPPA^+$-$TCPB^-$. EPR modulation amplitude, 0.05 mT. (e) In situ electrolysis in an electrochemical EPR cell (see Experimental Section) of 5.4 mM TTF with 0.1 M *n*-Bu_4NPF_6. EPR modulation amplitude, 0.05 mT. (f) In situ electrolysis in a liquid/liquid electrochemical EPR cell by polarization of the water/DCE interface of 5 mM TTF with 50 mM $BTPPA^+TCPB^-$. EPR modulation amplitude, 0.05 mT.

Lines a−d of Figure 4 illustrate the EPR spectra that were obtained for $TCNQ^{-\bullet}$ in DCE under various experimental conditions using different generation methods and different concentrations of TCNQ. The spectrum in Figure 4a is of $TCNQ^{-\bullet}$ that was generated electrochemically from a 5 mM solution of TCNQ (0.1 M *n*-Bu_4NPF_6) using an in situ stationary solution electrochemical EPR cell (see Experimental Section) where there is only a partial conversion of the TCNQ to $TCNQ^{-\bullet}$. The spectrum in Figure 4b is of 5 mM $TCNQ^{-\bullet}$ (0.1 M *n*-Bu_4NPF_6) that was generated from TCNQ in a controlled-potential electrolysis cell (see Experimental Section) so that there was >99% $TCNQ^{-\bullet}$ (compared to TCNQ). Figure 4c is the spectrum of $TCNQ^{-\bullet}$ that was obtained when the solution from Figure 4b was diluted to give a concentration of 0.1 mM $TCNQ^{-\bullet}$ (2 mM *n*-Bu_4NPF_6). The insensitivity of the line width of the EPR signals to the concentration of $TCNQ^{-\bullet}$ and ratio of TCNQ to $TCNQ^{-\bullet}$ suggests that the line broadening is possibly due to strong ion pairing between $TCNQ^{-\bullet}$ and the supporting electrolyte cation in the low relative permittivity medium causing anisotropic slow rotation. There was no evidence of a precipitate forming in any of the experiments illustrated in Figure 4a−c; thus exchange narrowing from a solid radical is an unlikely explanation for the broad lines. Similar to $TCNQ^{-\bullet}$, the $TTF^{+\bullet}$ radical cation gave a single-line EPR spectrum ($\Delta H_{pp} = 0.3$ mT) when electrolyzed in an in situ stationary solution electrochemical EPR cell (Figure 4e).

Voltammetric experiments were next carried out with the four-electrode potentiostat using the cylindrical cell containing both

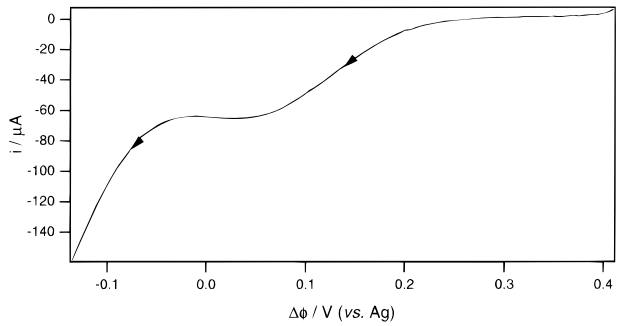

Figure 5. A linear sweep voltammogram obtained at a sweep rate of 0.024 V s^{-1} on the polarization of the interface between DCE, containing TCNQ (0.87 mM) and BTPPA TPBCl (10 mM), and water containing $K_4Fe(CN)_6$ (0.4 M), $K_3Fe(CN)_6$ (10 mM), and Li_2SO_4 (1 M). The aqueous reference electrode was Ag_2SO_4/Ag while the organic reference electrode was Ag/AgCl/aqueous LiCl (10 mM) with BTPPA Cl (1 mM). Pt wires were used as counter electrodes in both phases.

potassium ferrocyanide and potassium ferricyanide in the aqueous phase along with TCNQ dissolved in DCE. Figure 5 shows a linear sweep voltammogram obtained for the reduction of oil-phase TCNQ at the water/DCE interface by aqueous potassium ferrocyanide. The voltammetric wave shown in Figure 5 is consistent with a one-electron reduction of TCNQ to $TCNQ^{-\bullet}$ limited by the diffusion of TCNQ to the interface [24] (the aqueous phase contains an excess of both potassium ferrocyanide and ferricyanide). The half-wave potential of the $TCNQ^{-\bullet}$ ion transfer from DCE to water is 0.2 V more positive than the electron transfer from ferrocyanide to TCNQ.[24b] Therefore, care was taken to remain outside the potential region where ion transfer occurred during potential step experiments. Similar voltammetric behavior was found for the oxidation at the ITIES of organic phase TTF by aqueous potassium ferricyanide.

The voltammetric experiments were then repeated with the flat liquid/liquid cell with the EPR data being recorded simultaneously (see experimental section for more details). Figure 4d and Figure 4f show the EPR spectra that were obtained during the reduction of TCNQ and oxidation of TTF, respectively, in the liquid/liquid electrochemical EPR cell. In both cases the signals obtained had very similar line widths to the signals obtained from conventional electrolysis experiments which, in the absence of hyperfine structure, is good evidence that the radicals are $TCNQ^{-\bullet}$ and $TTF^{+\bullet}$. Figure 6 shows the raw EPR and current data obtained from potential step experiments on the TTF/ferricyanide system under different time regimes, with the interval between the potential steps ranging from $t = 2$ s to $t = 10$ s. The EPR data were obtained by overmodulating the signal response for $TTF^{+\bullet}$ and holding the magnetic field at a constant value corresponding to the maximum signal intensity. In each case, a reducing potential difference was first applied across the water/DCE interface for several seconds in order to convert any $TTF^{+\bullet}$ present at the interface back to neutral TTF by heterogeneous electron transfer from the aqueous phase. Figure 6 shows that the application of an oxidizing potential difference ($\Delta\phi_1$, from $t = 0$) led to an immediate increase in the positive current flowing which then began to decay with time as would be expected for a charge-transfer reaction governed by diffusion of the reactants, while simultaneously the EPR signal rose continually over the time

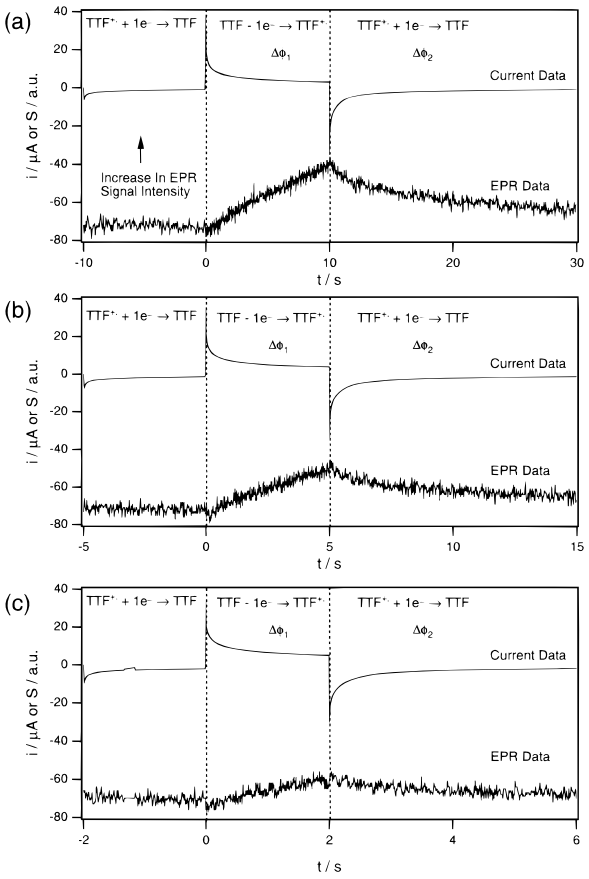

Figure 6. EPR and current data recorded simultaneously during the oxidation and reduction of TTF or $TTF^{+\bullet}$, respectively, obtained using the liquid/liquid four-electrode flat electrochemical cell shown in Figure 2 during potential step (chronoamperometry) experiments. The organic phase (DCE) contained 5 mM TTF and 50 mM $BTPPA^+$-$TCPB^-$. The aqueous phase contained 30 mM $K_4[Fe(CN)_6]$, 30 mM $K_3[Fe(CN)_6]$, and 0.1 M Li_2SO_4. The potential difference imposed to induce oxidation of TTF was +0.3 V ($\Delta\phi_1$), while this process was reversed using a potential difference of −0.3 V ($\Delta\phi_2$), vs the Ag wire reference electrodes. Plots a−c represent different time scales for the experiments. The EPR data were obtained by overmodulating and recording the signal intensity at a constant magnetic field corresponding to a maximum absorbance. EPR modulation amplitude, 0.5 mT.

frame of the experiment, due to an increase in concentration of $TTF^{+\bullet}$. Conversely, when a reducing potential difference ($\Delta\phi_2$) was applied across the water/DCE interface, a large negative current was initially observed, which subsequently fell with time, while concomitantly the EPR signal decreased in intensity due to the interfacial reduction of $TTF^{+\bullet}$ back to TTF.

The EPR cavity is spatially discriminating; thus, the position of the radical species in the cavity is critical in determining the signal intensity. For this reason, the liquid/liquid interface was positioned as close to the center of the TE_{102} cavity as possible, where there is the greatest sensitivity. If the diffusion coefficient of the radical ions is estimated to be 5×10^{-6} cm^2 s^{-1}, then in the time scale of the experiments illustrated in Figure 6, the distance diffused by the radicals is insufficient for the $\cos^2$ sensitivity of the cavity to be important (in 60 s the radical ions will diffuse <0.1 mm^2 from the interface). In addition, providing the time frame of the experiment is relatively short (<1−2 min), natural convection does not come into effect, which would otherwise result

in a distortion of the relative signal intensity.[25] Therefore, because all experiments were conducted on a short time scale (<60 s), the intensities of the EPR signals shown in Figure 6 are directly proportional to the concentration of the radical species present. Figure 6 also shows that EPR data with a reasonable signal-to-noise ratio could be obtained at time scales down to approximately 2 s (Figure 6c), although with signal-averaging techniques, shorter time periods would undoubtedly be possible. Use of higher concentrations of parent molecules would allow greater sensitivity for shorter time-scale experiments. With the present experimental arrangement, concentrations of parent molecules can be decreased to approximately 0.1 mM and still maintain adequate signal-to-noise EPR transient data, at least for the longer time-scale experiments ($10 < t/\mathrm{s} < 60-120$).

The transient signal response can be quantitatively analyzed because the normalized EPR signal (S) is proportional to the total radical concentration (C_{rad}) at short times (<1−2 min). For large changes in C_{rad}, EPR line-broadening effects must be taken into consideration. This proportionality can thus be extended to S and the total charge passed (Q) across the interface;

$$\frac{S}{S_0} = \frac{Q}{z_{rad}F} = \frac{1}{z_{rad}F}\int_0^{\tau} i_d(t)\,\mathrm{d}t \qquad (3)$$

where S_0 is the signal that would be obtained if 1 mol of radical were located at the cavity center, z_{rad} is the charge on the radical ion formed, Q is the total charge passed, i_d is the diffusion-limited current, τ is the duration of the radical generating potential pulse, and F is the Faraday constant. The charge passed as a function of time may be found by integrating the Cottrell equation with respect to time under diffusion-only conditions,[26]

$$i_d(t) = \frac{nFAD^{1/2}C}{\pi^{1/2}t^{1/2}} \qquad (4)$$

where C in eq 4 is the bulk concentration of the analyte. Hence the transient signal response may be found by combining eq 3 and the integrated form of eq 4.

Figure 7 shows the EPR data obtained from the experiments illustrated in Figure 6 which have been analyzed in a way analogous to chronocoulometric data. The EPR signal intensity data (S) corresponding to the oxidation of TTF to $TTF^{+\bullet}$ is plotted as a function of $t^{1/2}$ while the signal intensity data for the reduction of $TTF^{+\bullet}$ to TTF is plotted as a function of Θ [$\Theta = t^{1/2} - (t - \tau)^{1/2}$].[27a,28] The graphs in Figure 7 show that the analyzed data agree very well with theory as the plots are linear, have very similar slopes, and intercept close to zero signal intensity. The ordinate axis intercept (S-intercept) and the slopes of the graphs are given in Figure 7. The observation that the S vs Θ plots (for $TTF^{+\bullet} + 1e^- \rightarrow TTF$) intercept the ordinate axis close to zero EPR signal intensity for $TTF^{+\bullet}$ (and $TCNQ^{-\bullet}$) suggests that the EPR transient data are not complicated by ion transfer of $TCNQ^{-\bullet}$ or $TTF^{+\bullet}$ into the aqueous phase. Also, it was noted optically that the intense colors associated with the organic radical species were only detected in the organic phase.

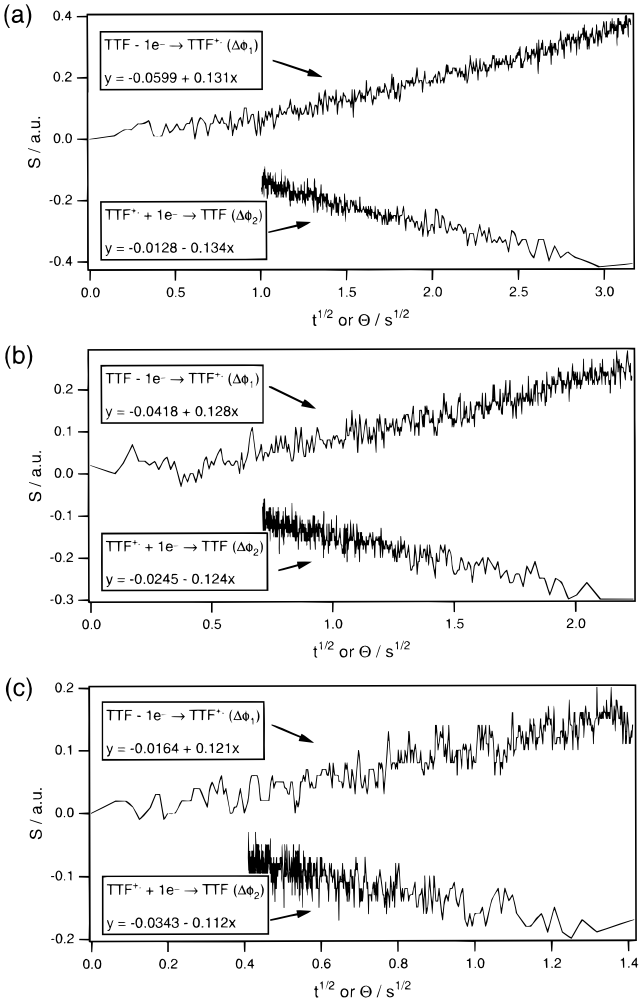

Figure 7. Plots of $t^{1/2}$ or Θ [$\Theta = t^{1/2} - (t - \tau)^{1/2}$, where τ is the duration of the forward phase] vs the EPR signal intensity recorded during potential jump experiments for the oxidation and reduction of TTF or $TTF^{+\bullet}$, respectively, and obtained using the liquid/liquid four-electrode flat electrochemical cell shown in Figure 2. The plots shown in (a−c) represent different time scales for the experiments and correspond to the raw EPR data shown in Figure 6. The experimental conditions are identical with those given in Figure 6. In the boxed insets, y denotes the ordinate axis and x denotes the abscissa.

An estimation of the lower bound on the rate constant of the heterogeneous charge-transfer reaction can be made from the S vs $t^{1/2}$ data (Figure 7) by noting that finite kinetics would cause a delay in the rise of the signal which would result in a negative signal axis intercept. Writing the standard chronocoulometric expression[27b] in terms of EPR signal intensity rather than charge leads to the following expression:

$$\frac{S}{S_0} = k_f CA\left(\frac{2t^{1/2}}{\lambda\pi^{1/2}} - \frac{1}{\lambda^2}\right) \qquad (5)$$

where A is the interfacial area, k_f is the pseudo-first-order rate constant for the "forward" (radical generating process), and the parameter λ is given by

(25) Goldberg, I. B.; Bard, A. J. *J. Phys. Chem.* **1971**, *75*, 3281.
(26) Cottrell, F. G. *Z. Phys. Chem.* **1902**, *42*, 385.
(27) Bard A. J.; Faulkner, L. R. *Electrochemical Methods*; Wiley: New York, 1980: (a) p 603; (b) p 205; (c) p 218.
(28) Jeanmaire, D. L.; Van Duyne, R. P. *J. Electroanal. Chem.* **1975**, *66*, 235.

$$\lambda = \left(\frac{k_f}{D^{1/2}} + \frac{k_b}{D^{1/2}}\right) \quad (6)$$

with k_b representing the rate constant for the reverse process. Comparison of the gradient and intercept of the S vs $t^{1/2}$ plots yields the conclusion that k_f must be at least 5×10^{-3} cm s^{-1}, the process being pseudo first order because of the large excess of the aqueous phase-redox couple. The minimum second-order interfacial rate constant is thus 200 mol^{-1} cm^4 s^{-1}, as the concentration of the aqueous-phase species was 0.03 M. This can be compared with a recent experimental study which found the rate constant for electron transfer between ferrocene and ferrocene carboxylate at the ITIES to be 600 mol^{-1} cm^4 s^{-1}.[29]

While the EPR data shown in Figure 6 is undistorted by ohmic drop effects, the transient voltammetric data show a considerable departure from ideality because of a combination of the high resistivity of the organic phase and the restricted electrode geometry in the flat cell. Figure 8 shows the current−time curves obtained via potential step experiments in the flat cell which have been analyzed by plotting current vs $t^{-1/2}$ according to the Cottrell expression (see eq 4) for the generation of $TCNQ^{-\bullet}$ via the one-electron reduction of TCNQ. For the reverse reaction where $TCNQ^{-\bullet}$ is oxidized back to TCNQ, the current has been plotted as a function of θ, according to the relation[30]

$$-i_r(t) = i_d(t) = \frac{nFAD^{1/2}C}{\pi^{1/2}}\left[\frac{1}{(t-\tau)^{1/2}} - \frac{1}{t^{1/2}}\right] \quad (7)$$

where θ is the quantity in brackets in eq 7. Panels a and b of Figure 8 show the effect the position of the organic-phase reference electrode had on the current response for potential step measurements performed in the flat cell. In Figure 8a, the organic phase reference electrode was positioned 10 mm from the ITIES, while the reference electrode−interface separation was 1 mm in Figure 8b. The plots given in Figure 8b are closer to the response predicted by the Cottrell equation, although they are still not ideal. Inspection of Figure 8c shows that a linear current-$t^{-1/2}$ response (in agreement with eq 4) could be obtained when voltammetric experiments were performed in a cylindrical liquid/liquid cell (see Experimental Section). Analysis of the gradient of the plots in Figure 8c allowed an estimation of the diffusion coefficient of TCNQ (according to eq 4) in DCE of 6.9×10^{-6} cm^2 s^{-1}. By comparison, the data recorded using the flat cell required for compatibility with EPR spectroscopy (Figure 8a and b) showed nonlinear Cottrell plots and the estimated diffusion coefficients from these plots were markedly lower than those obtained in the cylindrical cell. This effect is principally due to the enhanced resistance imposed by the flat cell geometry causing the faradaic current to be obscured by a significant charging process, thus resulting in a lowering of the calculated diffusion coefficient values. Such effects are common in electrochemical experiments at the ITIES with experimental data from micrometer-scale liquid/liquid interfaces retaining a considerable nonfaradaic component,[31] despite the reduced capacitance of these interfaces. As noted above, the spectroscopic data is are apparently free of such distortions and thus present a promising future pathway for the extraction of kinetic data from electron-transfer experiments at the ITIES.

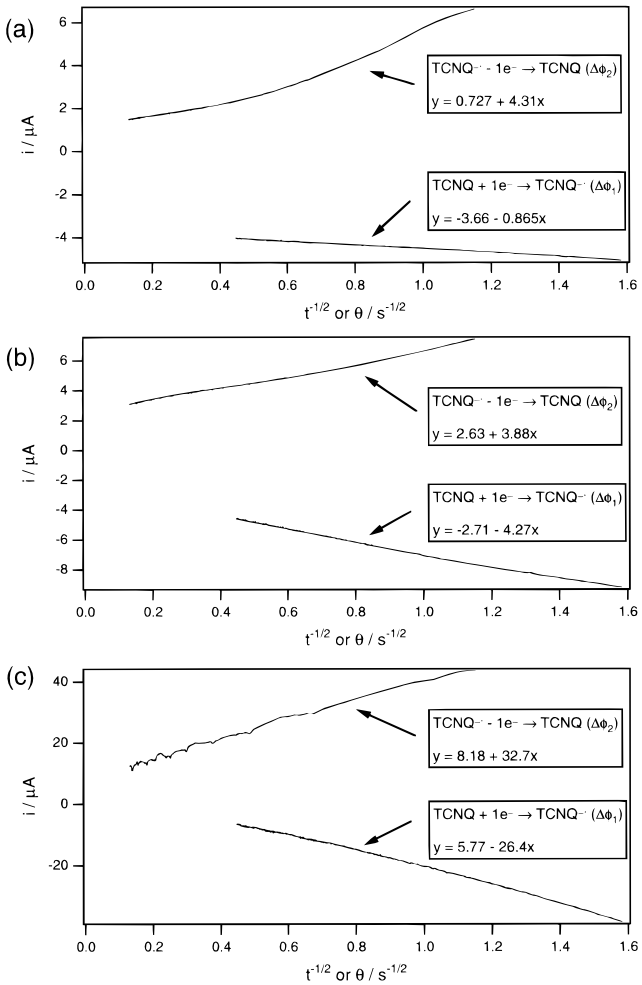

Figure 8. Current recorded during potential jump experiments vs $t^{-1/2}$ or θ [$\theta = (t-\tau)^{-1/2} - t^{-1/2}$, where τ is the duration of the forward phase] for the reduction and oxidation of TCNQ or $TCNQ^{-\bullet}$, respectively, at the ITIES. The potential difference imposed to induce reduction of TCNQ was −0.5 V ($\Delta\phi_1$), while this process was reversed using a potential difference of +0.3 V ($\Delta\phi_2$), vs a Ag wire reference electrode. The data were obtained using the liquid/liquid electrochemical EPR cell shown in Figure 2. The organic phase (DCE) contained 5 mM TCNQ and 50 mM $BTPPA^+TCPB^-$. The aqueous phase contained 30 mM $K_4[Fe(CN)_6]$, 30 mM $K_3[Fe(CN)_6]$, and 0.1 M Li_2SO_4. In the boxed insets, y denotes the ordinate axis and x denotes the abscissa. (a) The organic-phase reference electrode was positioned 10 mm from the liquid/liquid interface. (b) The organic-phase reference electrode was positioned 1 mm from the liquid/liquid interface. (c) Data were obtained in a cylindrical "low"-resistance liquid/liquid cell with an interface diameter of 1 cm. The organic phase (DCE) contained 0.25 mM TCNQ and 50 mM $BTPPA^+TCPB^-$. The aqueous phase contained 30 mM $K_4[Fe(CN)_6]$, 30 mM $K_3[Fe(CN)_6]$, and 0.1 M Li_2SO_4.

(2) Liquid/Liquid Voltammetric and EPR Studies on TCBQ and TFBQ and Their Associated Anion Radicals. Having established that transient EPR data obtained in the liquid/liquid electrochemical EPR cell could be modeled analogously to chronoamperometric data according to the Cottrell equation,

(29) Wei, C.; Bard A. J.; Mirkin, M. V. *J. Phys. Chem.* **1995**, *99*, 16033.
(30) Kambara, T. *Bull. Chem. Soc. Jpn.* **1954**, *27*, 523.
(31) Kontturi, A.-K.; Kontturi, K.; Murtomäki, L.; Quinn, B.; Cunnane, V. J. *J. Electroanal. Chem.* **1997**, *424*, 69.

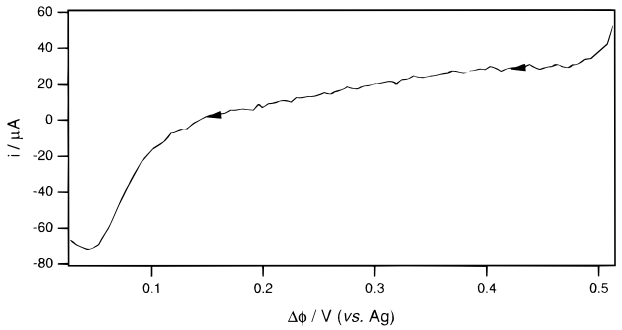

Figure 9. A linear sweep voltammogram obtained at a sweep rate of 0.25 V s^{-1} on the polarization of the interface between DCE, containing TCBQ (0.43 mM) and BTPPA TPBCl (25 mM), and water, containing $K_4Fe(CN)_6$ (0.27 M), $K_3Fe(CN)_6$ (0.27 M), and Li_2SO_4 (0.67 M). The aqueous reference electrode was Ag_2SO_4/Ag and the organic reference electrode was Ag/AgCl/aqueous LiCl (10 mM) with BTPPA Cl (1 mM). Pt wires were used as counter electrodes in both phases.

attention was turned to examining the liquid/liquid electrochemical EPR behavior of the two quinones, TCBQ and TFBQ, as model compounds for transmembrane electron transfer in biological systems. First, liquid/liquid electrochemical experiments were carried out using the relatively low resistance cylindrical cell containing an excess of both potassium ferrocyanide and potassium ferricyanide in the aqueous phase over the concentration of TCBQ dissolved in DCE. Linear sweep voltammetry in this cell produced a voltammetric wave close to the end of the potential window which is shown in Figure 9. The voltammetric wave obtained was consistent with the transfer of a negative charge from the aqueous phase to the organic phase and thus attributable to a net one-electron reduction of TCBQ by potassium ferrocyanide. Analysis of the dependence of the peak current on sweep rate (according to eq 8[27c]) allowed the calculation of a value for the diffusion coefficient of TCBQ in DCE of 6.1×10^{-6} cm^2 s^{-1} (where v in eq 8 is the scan rate).

$$i_p = 0.4463nFAC(nF/RT)^{1/2}\nu^{1/2}D^{1/2} \qquad (8)$$

The half-wave potential of the electron-transfer wave due to ferrocyanide/TCBQ was 0.06 V less positive than that of the ferrocyanide/TCNQ system, which corresponds exactly to the difference in formal reduction potentials quoted for TCBQ[18] and TCNQ[24c] in DCE.

The interfacial reduction of TCBQ was repeated in the flat cell with simultaneous measurement of the EPR spectrum seen on polarization of the ITIES. A single-line EPR spectrum with $\Delta H_{pp} = 0.12$ mT was obtained when sufficiently negative $\Delta\phi$ values were applied [Figure 10c (ii)]. A spectrum with a very similar ΔH_{pp} was also obtained when TCBQ was electrolyzed in a stationary solution in situ electrochemical EPR cell (see Experimental Section) [Figure 10c (i)]. The absence of hyperfine structure could be due either to quadrupolar broadening effects associated with the four equivalent Cl nuclei ($I = {}^3/_2$)[32] or signal-broadening effects associated with anisotropic slow tumbling (as observed for $TCNQ^{-\bullet}$ and $TTF^{+\bullet}$). No evidence was obtained of a precipitate forming; thus an exchange-narrowed solid radical species is

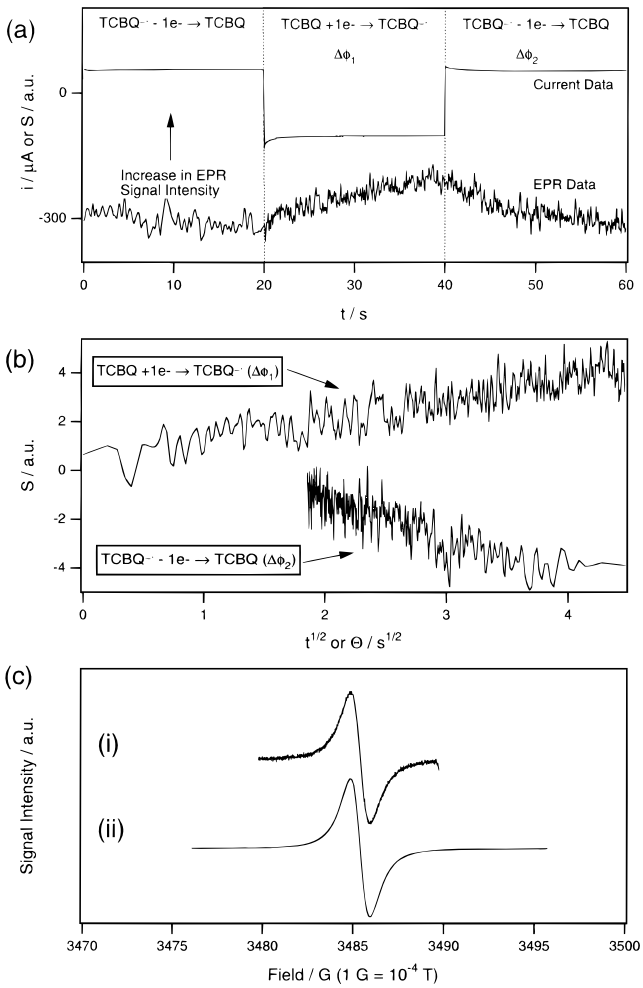

Figure 10. (a) EPR and current data recorded simultaneously during the reduction and oxidation of TCBQ or $TCBQ^{-\bullet}$, respectively, obtained using the liquid/liquid four-electrode flat electrochemical cell shown in Figure 2 during potential step (chronoamperometry) experiments. The organic phase contained 1.72 mM TCBQ and 0.1 M *n*-Bu_4NPF_6, and the aqueous phase contained $K_4Fe(CN)_6$ (0.27 M), $K_3Fe(CN)_6$ (0.27 M), and Li_2SO_4 (0.67 M). The potential difference imposed to induce reduction of TCBQ was −0.4 V ($\Delta\phi_1$), while this process was reversed using a potential difference of 0.0 V ($\Delta\phi_2$), vs the Ag wire reference electrodes. (b) Plot of $t^{1/2}$ or Θ [$\Theta = t^{1/2} - (t - \tau)^{1/2}$, where τ is the duration of the forward phase] verses the EPR signal intensity for raw EPR data shown in (a). The EPR data were obtained by overmodulating and recording the signal intensity at a constant magnetic field corresponding to a maximum absorbance. EPR modulation amplitude, 0.2 mT. (c) EPR spectra obtained in DCE by (i) in situ electrolysis in an electrochemical EPR cell (see Experimental Section) of 5.0 mM TCBQ with 0.1 M *n*-Bu_4NPF_6. Modulation amplitude, 0.02 mT. (ii) In situ electrolysis in a liquid/liquid electrochemical EPR cell by polarization of the water/DCE interface of 1.72 mM TCBQ with 0.1 M *n*-Bu_4NPF_6. EPR modulation amplitude, 0.02 mT.

unlikely. The EPR spectrum of the neutral radical (TCBQ-H$^\bullet$), which would be formed if proton transfer accompanied electron transfer at the ITIES, would clearly contain a proton splitting. However, the proton splitting may be masked by broadening, so the formation of TCBQ-H$^\bullet$ cannot be ruled out on the basis of the EPR data alone. However, the net charge observed in the cylindrical liquid/liquid cell was consistent with one electron being transferred from the water phase to the oil phase. If TCBQ-H$^\bullet$

(32) Corvaja, C.; Pasimeni, L.; Brustolon, M. *Chem. Phys.* **1976**, *14*, 177−182.

were being formed, then the net charge would be zero because the water to oil phase proton transfer would balance the electron transfer. Furthermore, the growth and decay of the EPR signal during potential jump experiments, when the EPR signal intensity was monitored at constant field, showed a time dependence similar to that of $TCNQ^{-\bullet}$ and $TTF^{+\bullet}$. The EPR signal increased in intensity as a potential difference ($\Delta\phi_1$) sufficient to cause the transfer of an electron from the aqueous-phase ferrocyanide to the oil-phase TCBQ was applied (Figure 10a). Conversely, when an oxidizing potential difference ($\Delta\phi_2$) sufficient to cause the transfer of an electron from oil-phase $TCBQ^{-\bullet}$ to the water-phase ferricyanide was applied, the EPR signal decreased in intensity (Figure 10a). Analysis of the $TCBQ^{-\bullet}$ transient EPR data in a manner analogous to the $TCNQ^{-\bullet}$ and $TTF^{+\bullet}$ data by plotting the signal intensity as a function of $t^{1/2}$ or Θ (Figure 10b) gave plots that were linear and intercepted close to zero EPR signal intensity. Therefore, the combination of the electrochemical and spectroscopic data implies that the initial product of TCBQ reduction at the ITIES is the one-electron-reduced product, $TCBQ^{-\bullet}$. The close similarity between the $TCBQ^{-\bullet}$, $TCNQ^{-\bullet}$, and $TTF^{+\bullet}$ transient EPR data obtained during potential jump experiments indicates that the TCBQ data do not appear to be complicated by ion transfer of $TCBQ^{-\bullet}$ into the water phase.

The behavior of TFBQ at the ITIES was also investigated by in situ liquid/liquid electrochemical EPR experiments. The reduction potential of TFBQ has been quoted as 50 mV less positive than that of TCBQ,[33] and both molecules display similar voltammetric behavior in terms of the number of reduction processes and the stability of their associated radicals formed by one-electron reduction. One advantage of studying the TFBQ system over the TCBQ system is that TFBQ contains four equivalent F nuclei with $I = {}^1/_2$; thus the EPR spectra of its associated anion radical are not susceptible to quadrupolar line-broadening effects. Therefore, this leads to the possibility that any radicals detected during the reduction of TFBQ could be unequivocally assigned to $TFBQ^{-\bullet}$ if the hyperfine splitting constants matched that of the known anion radical. Figure 11a shows the EPR spectrum that was obtained via reduction of TFBQ in DCE in a stationary solution electrochemical EPR cell. Figure 11b shows the EPR spectrum that was obtained by reduction of oil-phase TFBQ at the water/oil interface by water-phase potassium ferrocyanide in the liquid/liquid flat cell. The spectra in Figure 11a and b are very similar and allow the calculation of the hyperfine splitting constant for the F atoms of 0.396 mT, which is in good agreement with published data.[34,35] This result provides further strong evidence that semiquinones are stable at the water/oil interface. Also, there was no evidence of the monoprotonated quinone (TFBQ-H$^\bullet$) being formed, which has a distinctive EPR spectrum.[35]

(33) Peover, M. E. *J. Chem. Soc.* **1962**, 4540.
(34) Eastman, J. W. Androes, G. M.; Calvin, M. *Nature* **1962**, 1069.
(35) Hudson, A.; Lewis, J. W. *J. Chem. Soc. B* **1969**, 531.

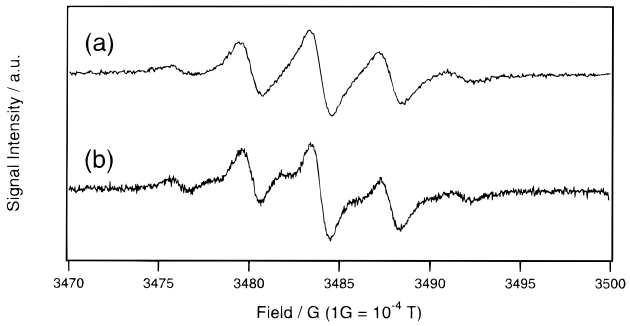

Figure 11. EPR signals obtained during the electrolysis of TFBQ in DCE: (a) In situ electrolysis in an electrochemical EPR cell (see Experimental Section) of 5.2 mM TFBQ with 0.1 M *n*-Bu_4NPF_6. Modulation amplitude, 0.1 mT. (b) In situ electrolysis in a liquid/liquid electrochemical EPR cell by polarization of the water/DCE interface of 7.6 mM TFBQ with 0.1 M *n*-Bu_4NPF_6. EPR modulation amplitude, 0.1 mT.

CONCLUSION

The performance of a simple and robust liquid/liquid electrochemical EPR cell has been quantified using TCNQ and TTF in the oil phase as electron acceptors or donors, respectively, for the aqueous-phase ferricyanide/ferrocynanide redox couple. The EPR signal intensity (at constant magnetic field) obtained by applying a $\Delta\phi$ value sufficient to produce the radical anion ($TCNQ^{-\bullet}$) or cation ($TTF^{+\bullet}$) by one-electron transfer across the water/DCE interface was found to exhibit Cottrell-type behavior. The EPR signal decayed or increased in intensity as a function of time ($t < 1$ min) after potential difference ($\Delta\phi$) step experiments, as expected for a diffusion-controlled heterogeneous electron-transfer reaction. However, the design of the liquid/liquid cell for optimal spectroscopic performance meant that current data obtained simultaneously was of limited value due to high ohmic resistance.

In situ experiments in the liquid/liquid electrochemical EPR cell have shown that the electron transfer from the water phase to a quinone (TCBQ and TFBQ) in an oil phase (DCE) results in a stable radical being formed. The hyperfine splitting in the $TFBQ^{-\bullet}$ radical provided unambiguous evidence that an unprotonated semiquinone radical was being formed. The behavior of the quinone molecules following electron transfer at liquid interfaces has interesting consequences for studies of electron transfer within biological membranes.

ACKNOWLEDGMENT

R.D.W. thanks the Ramsay Memorial Fellowships Trust for a Postdoctoral Fellowship and Wadham College, Oxford, for a Lectureship. R.A.W.D. gratefully thanks the Royal Commission for the Exhibition of 1851 for the award of a Research Fellowship.

Received for review July 29, 1997. Accepted December 2, 1997.

AC9708147